Forest and Society
Vol. 7(1): 116-134, April 2023
doi: 10.24259/fs.v7i1.22062

REGULAR RESEARCH ARTICLE

Estimation and Mapping Above-Ground Mangrove Carbon Stock Using Sentinel-2 Data Derived Vegetation Indices in Benoa Bay of Bali Province, Indonesia

A. A. Md. Ananda Putra Suardana [1, *], Nanin Anggraini [2], Muhammad Rizki Nandika [1], Kholifatul Aziz [3], Abd. Rahman As-syakur [4, 5], Azura Ulfa [2], Agung Dwi Wijaya [3], Wiji Prasetio [2], Gathot Winarso [2], Ratih Dewanti Dimyati [2]

AFFILIATIONS

1. Research Center for Oceanography, National Research and Innovation Agency (BRIN), Jakarta, Indonesia
2. Research Center for Remote Sensing, National Research and Innovation Agency (BRIN), Jakarta, Indonesia
3. Center for Data and Information, National Research and Innovation Agency (BRIN), Jakarta, Indonesia
4. Center for Remote Sensing and Ocean Science (CReSOS), Udayana University, Denpasar, Indonesia
5. Marine Science Department, Faculty of Marine and Fisheries, Udayana University, Denpasar, Indonesia

*Corresponding author: anandayobi@gmail.com

RECEIVED 2022-08-08
ACCEPTED 2023-02-24

ABSTRACT

Carbon dioxide (CO_2) is one of the greenhouse gases that cause global warming, with the highest atmospheric concentration. Mangrove forests absorb CO_2 three times higher than terrestrial forests and tropical rainforests. Moreover, mangrove forests can be a source of Indonesian income in the form of a blue economy. Therefore, an accurate method is needed to investigate mangrove carbon stock. The utilisation of remote sensing data with the results of the above-ground carbon (AGC) detection model of mangrove forests based on multispectral imaging and vegetation index can be a solution to obtain fast, cheap, and accurate information related to AGC estimation. This study aimed to investigate the best model for estimating the AGC of mangroves using Sentinel-2 imagery in Benoa Bay, Bali Province. The Random Forest (RF) method was used to classify the difference between mangrove and non-mangrove by treating several parameters. Furthermore, a semi-empirical approach was used to assess and map the AGC of mangroves. Allometric equations were used to calculate and produce AGC per species. Moreover, the model was built with linear regression equations for one variable x and multiple regression equations for more than one x variable. Root Mean Square Error (RMSE) was used to assess the validation of the model results. The results of the mangrove forests area detected in the research location around 1,134.92 ha, with an Overall Accuracy (OA) of 0.984 and a kappa coefficient of 0.961. This study highlights that the best model was the combination of IRECI and TRVI vegetation indices (RMSE: 11.09 Mg/ha) for a model based on red edge bands. Meanwhile, the best results from the model that does not use the red edge band were the combination of TRVI and DVI vegetation indices (RMSE: 13.63 Mg/ha). The use of red edge and NIR bands is highly recommended in building the AGC model of mangrove forests because they can increase the accuracy value. Thus, the results of this study are highly recommended in estimating the AGC of mangrove forests because it has been proven to increase the accuracy value of previous studies using optical images.

KEYWORDS

Carbon stock; Mangrove forests; Sentinel image; Model; Vegetation indices; Coastal zone.

1. INTRODUCTION

Mangrove forests, as one of the main ecosystems in coastal areas, have many important roles, both from an ecological, biological and physical perspective. Ecologically, mangrove plays an important role in providing benefits and services related to carbon sequestration (Fourqurean et al., 2019; Sidik et al., 2019). Mangrove forests can store large amounts of carbon in vegetation (biomass) and other organic materials (Alongi, 2012).

According to FAO (2007) data, the area of mangrove forests in Indonesia from 1980 to 2005 decreased from 4.2 million ha to 2.9 million ha. The decline in mangrove areas was largely due to human activities such as converting mangrove forest areas into fish or shrimp ponds and urban development (Richards & Friess, 2016). The loss of mangrove forests accounts for 42% of Southeast Asia's global carbon dioxide (CO_2) emissions from mangrove damage (Murdiyarso et al., 2015).

Information on CO_2 absorption from mangrove forests is essential in solving emissions or air pollution issues, particularly in urban areas. Determine the level of CO_2 emissions absorbed by mangrove forests can be done by estimating the total carbon stock contained in the mangrove biomass (Hastuti et al., 2017; Suardana et al., 2022). According to Heumann (2011), combining mangrove forest biomass estimation data with remote sensing data was the best and most practical method. This combination produced an allometric equation, forming the basis for an estimation model for mangrove forest carbon stocks (Wicaksono et al., 2011; Hirata et al., 2014; Patil et al., 2015).

Benoa Bay mangrove was one of the mangrove forests in strategic urban Bali areas. The study of above-ground carbon (AGC) estimation in mangrove forests using remote sensing with a vegetation index in Benoa Bay needs to better studied. Previous research proposed by Dewanti et al., (2020) applied a systematic sampling method but had a long-time constraint and high costs, while research from Mahasani et al. (2021) used ALOS PALSAR satellite imagery but had moderate accuracy results. Hence, this study aimed to develop an AGC estimation model for mangrove forests based on multispectral imaging and a vegetation index. We hypothesise that the development of combined multispectral imaging and a vegetation index with a semi-empirical approach is the best model for estimating mangrove AGC.

2. MATERIALS AND METHODS

2.1 Study Site

The mangrove forest of Benoa Bay is geographically located in the south of Bali, divided into two regencies/cities, namely Denpasar City and Badung Regency (Figure 1). Mangrove forests grow across Benoa Bay in a strategic area of business growth centres and three main tourism areas: Nusa Dua, Sanur, and Kuta.

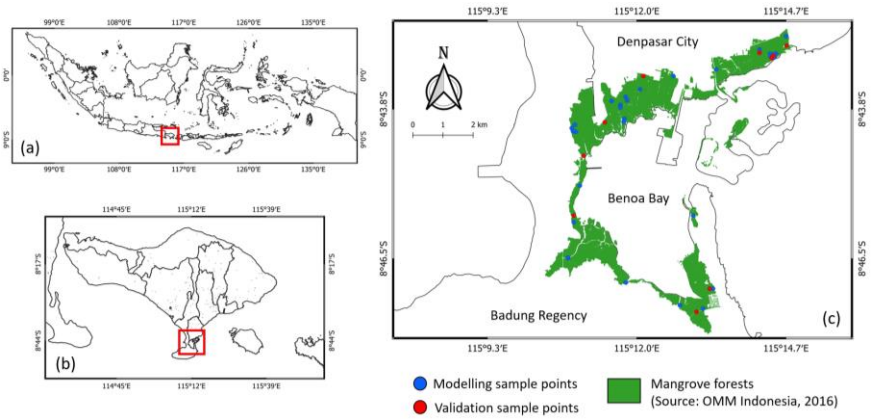

Figure 1. Study site: (a) The geographical location of Bali Province in Indonesia, (b) The geographical location of Benoa Bay in Bali Province, (c) Coastal study sites in Benoa Bay with mangrove forests extracted from Sentinel-2

Based on the Decree of the Minister of Forestry Number: 544/Kpts-II/1993 dated September 25, 1993, the mangrove forest area reaches 1,373.5 ha and is the largest mangrove forest in Bali Province. Previous studies showed three dominant mangrove genera in the mangrove forest of Benoa Bay, namely *Sonneratia sp.*, *Rhizophora sp.*, and *Bruguiera sp.* (Mahasani et al., 2021).

2.2 Methods

Details of the Sentinel-2 data utilisation method used to build the estimation model of Above-ground Carbon Stock in mangroves were schematically presented in Figure 2.

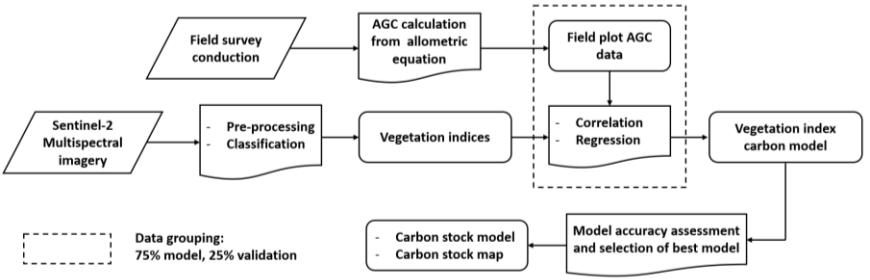

Figure 2. The flowchart of study methods used for mapping and calculating the AGC of mangrove forests

2.2.1 Data collection

The image utilised in this study was derived from Sentinel-2 MSI Level-2A data from the European Space Agency (ESA), which includes multispectral data that has completed the previous pre-processing stage (Table 1). The data was obtained from the Remote Sensing Research Center, National Research and Innovation Agency (BRIN), Indonesia's official institution in image data acquisition. The downloaded image was a Level 2A image product that has been ortho into the UTM/WGS84 projection. This product was generated using a Digital Elevation Model (DEM) to project the image into cartographic coordinates.

Table 1. Sentinel-2 satellite image specifications include spatial resolution and spectral resolution (ESA, 2012; ESA, 2015)

Spatial resolution (m)	Spectral resolution (nm)
10	Blue (~490 nm), Green (~560 nm), Red (~665 nm), NIR (~842)
20	Vegetation Red Edge (~705 nm, ~740 nm, ~783nm, ~865 nm), and SWIR (~1610 nm and ~2190 nm)
60	Coastal Aerosol (~443 nm), Water Vapour (~940 nm), and Cirrus band (~1375 nm)

2.2.2 Field data collection

Field data were collected from July 1st – 6th, 2022, considering this month was the dry season, so the field activities were not constrained by rain. The satellite image used was Sentinel 2-L2A composite with an acquisition period from January 2nd, 2021 to June 26th, 2022. The Sentinel 2-L2A satellite image set produces a cloud-free annual period composite. Another consideration was based on information from the Ngurah Rai Forest Park (Tahura Ngurah Rai). In 2021 – 2022 there were no significant changes in mangroves (1132 ha), so composite satellite imagery can be used.

In this study, 40 field points were taken with a division of 30 points (75%) to build the model and 10 points (25%) to validate the model. Creating these field points uses a random sampling method and is adjusted to the field conditions that consider

accessibility at each point. A 10-by-10-meter square plot was taken at each location. The plot size was adjusted to Sentinel-2 resolution of 10 meters. The transect line was made perpendicular to the shoreline or river to the mainland. The transect line was a modification of Kauffman & Donato (2012), which was previously in the form of a circle, while in this study, the plot was square, which adjusts the shape of the pixels in the remote sensing image (Figure 3).

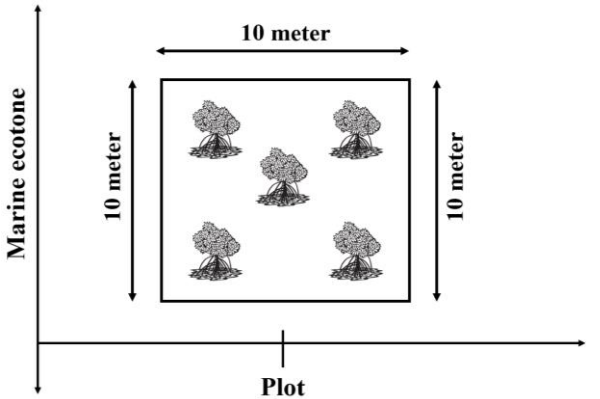

Figure 3. Schematic of plot layout for mangrove sampled (Source: modification from Kauffman & Donato, (2012))

Identification of mangrove species used an ecological approach by considering the characteristics of mangroves and growth zones. Meanwhile, DBH was measured in each plot for trees with a diameter of 10 cm because this size has a significantly contributes to the estimation of above-ground biomass (Brown, 2002). Diameter at breast height (DBH) was measured at the height of an adult's chest or approximately 1.3 meters from the ground. The calculation of DBH will be different for each condition, so that the measurement rules can be seen in Figure 4.

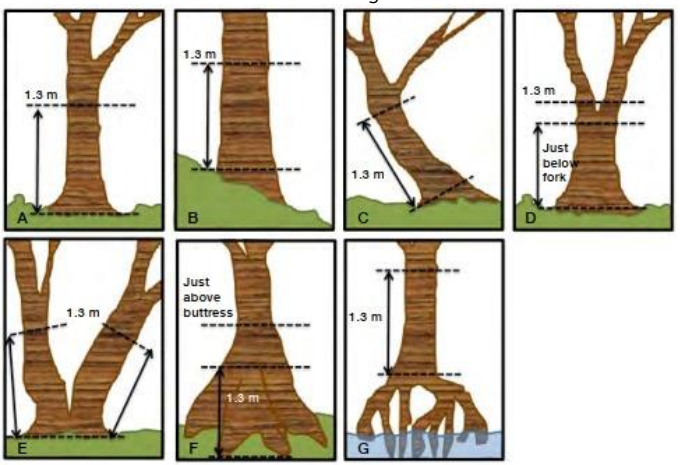

Figure 4. Estimating diameter at breast height (DBH) for irregular mangrove trees (Source: modified from Pearson et al., (2005))

2.2.3 Remote sensing data processing and image classification

Classifying mangroves and non-mangrove was carried out on the Google Earth Engine (GEE) platform. The Sentinel 2-L2A image set with less than 20% cloud cover produceed

a cloud-free annual period composite in the Benoa Bay area and its surroundings. The cloud masking process utilised the Quality Assessment (QA) band and the median reducer function available in GEE. The use of the QA band removes cloud contamination in each image, while the median reducer function was used to select the mean pixel value of the entire stack of images used. From these results, an image is generated to avoids pixel value that are too bright (e.g., clouds) or too dark (e.g., shadows).

Furthermore, the mangrove ecosystem's specific area of interest (AOI) was selected by masking using three parameters. These parameters included digital elevation model (DEM) less than 50 meters, Normalized Difference Vegetation Index (NDVI) greater than 0.25, and Modified Normalized Difference Water Index (MNDWI) greater than -0.5. The elevation model utilized the Shuttle Radar Topography Mission (SRTM) data available on the GEE platform. Assuming that mangroves grow and are detected in lowland areas, a DEM of less than 50 meters was chosen. At the same time, the NDVI and MNDWI indices were obtained through digital image transformation from Sentinel 2A data. The vegetation index used for the classification process in this study includes Simple Ratio (SR), NDVI, MNDWI, Green Chlorophyll Vegetation Index (GCVI), and Modular Mangrove Recognition Index (MMRI).

In this study, we used the random forest (RF) classification method to categorise the study site into two different land covers (mangrove and non-mangrove) through visual observation of false colour images (NIR, SWIR, Red). The RF algorithm is known for its high accuracy in predicting outcomes for classification and regression problems and is also robust against noise (Breiman, 2001; Rodriguez-Galiano et al., 2012). It achieves this by combining the predictions of multiple decision trees, and each trained on a different subset of the data. The decision to use RF is based on the fact that this algorithm can estimate the relative importance of each input feature, which can be helpful in feature selection and understanding the underlying factors contributing to the outcome. We classify using 100 decision trees, with five variables per split.

In many cases, 100 trees can be enough to achieve good performance with a random forest model, especially for smaller datasets and more straightforward problems. This was also stated by Oshiro et al., (2012) that an RF must have some trees between 64 – 128 trees. In addition, choosing five variables per split is because using a small number of variables can increase the diversity of trees in the forest, resulting in better performance on complex data sets. The number of variables per split determines how many features are considered at each decision tree split (Regier et al., 2023). When a smaller number of variables is selected, each tree is forced to consider a different subset of features, which increases the diversity of the trees in the forest. A spatial filter was built based on the “Connected Pixel Count” function in GEE to minimise errors in pixel sets. This function removes pixels not connected by an identical set of pixels. This filter takes at least ten connected pixels to reach the minimum connection value. The validation test in the classification process uses a confusion matrix, which is accurate in validating satellite and field image results (Han et al., 2012).

2.2.4 Calculation of Vegetation Indices

The NDVI is the most widespread vegetation indicator for calculating forest biomass (Li et al., 2007). However, using NDVI needs to accurately characterize forest biomass estimates or even carbon estimates (Foody et al., 2001). In this study, we compare and combine seven vegetation indices (Table 2) to build an estimation model for above-ground mangrove carbon stock including NDVI, Modified Red Edge-Simple Ratio (mRE-SR), Difference Vegetation Index (DVI), Inverted Red Edge Chlorophyll Index (IRECI), Red-Edge Simple Ratio (SRre), Chlorophyll Index Red Edge (Clre), and Total Vegetation Ratio Index (TRVI).

Table 2. Equations of vegetation indices used for above-ground mangrove carbon stock model development

Vegetation Indices	Equations	References
NDVI (Normalized Difference Vegetation Index)	$NDVI = \frac{NIR - Red}{NIR + Red}$	Ramdani et al., (2019); Pham et al., (2018); Rouse et al., (1973)
mRE-SR (Modified Red Edge-Simple Ratio)	$mRE\text{-}SR = \frac{\left(\frac{NIR}{Red\ Edge}\right) - 1}{\sqrt{\left(\frac{NIR}{Red\ Edge}\right)} + 1}$	Zhu et al., (2017); Pu & Landry, (2012)
DVI (Difference Vegetation Index)	$DVI = NIR - Red$	Hong Wei et al., (2019); Tucker, (1980)
IRECI (Inverted Red Edge Chlorophyll Index)	$IRECI = \frac{(NIR - Red)}{\left(\frac{Red\ Edge\ 1}{Red\ Edge\ 2}\right)}$	Clevers et al., (2000)
SRre (Red-Edge Simple Ratio)	$SRre = \frac{NIR}{Red\ Edge}$	Hallik et al., (2019); Jordan, (1969)
Clre (Chlorophyll Index Red Edge)	$Clre = \left(\frac{NIR}{Red\ Edge}\right) - 1$	Gitelson et al., (2003); Gitelson et al., (2006)
TRVI (Total Ratio Vegetation Index)	$TRVI = \sqrt{\frac{NIR}{Red}}$	Fadaei et al., (2012)

2.2.5 Estimation of Above Ground Carbon (AGC)

Before obtaining the AGC value, the above-ground biomass (AGB) of mangroves was calculated for each species found. The AGB calculation uses an allometric equation designed for use in Asian mangroves (Table 3), so it is very relevant to be used in Indonesia. Allometric equations can estimate mangrove biomass using the DBH parameter (Kumar & Mutanga, 2017).

Table 3. Allometric equations were used in this study to determine AGB (D is tree DBH in cm; ρ is wood density in g cm^{-3})

Species	Equation	Wood density (ρ)[a]	Reference
Bruguiera gymnorhiza	$0{,}0754 * \rho * D^{2{,}505}$	0.8683	Kauffman & Cole (2010)
Rhizophora apiculata	$0{,}043 * D^{2{,}63}$	0.8814	Komiyama et al., (2005)
Rhizophora mucronata	$0{,}128 * D^{2{,}60}$	0.8483	Fromard et al., (1998)
Sonneratia alba	$0{,}3841 * \rho * D^{2{,}101}$	0.6443	Fromard et al., (1998)
Xylocarpus granatum	$0{,}1832 * D^{2{,}2}$	0.6721	Komiyama et al., (2005)

Note: [a] World Agroforestry Center (2022)

AGC was computed from AGB based on the rules published in the Indonesian National Standard, (2011) 7724:2011, in which 0.47 or 47% of biomass is carbon. Fourqurean et al., (2019) calculate AGC with the following equation: $AGC = AGB * 0{,}47$.

2.2.6 AGC model development

In this study, the AGC estimation approach for one independent variable uses a linear regression model, while for more than one independent variable using a multiple regression model. The dependent variable was AGC, while the independent variable was a predetermined vegetation index. The best model will be selected from this processing based on the combination of the highest coefficient of determination (R^2) and the validation results with the lowest error.

2.2.7 Accuracy assessment and model validation

This study split the data into two groups: 25% for model validation and 75% for model construction. The coefficient of determination (R^2) is used to determine the model's accuracy, and the R^2 value of ≥ 0.8 is deemed to be high enough for the model to be run. The validation was performed on ten field data points (25%). AGC results from the model will be compared with field data as validation. The errors value is calculated using the Root Mean Square Error (RMSE). The advantage of RMSE is that it avoids taking the absolute value, which is undesirable in many mathematical calculations (Savage et al., 2013; Chai & Draxler, 2014).

3. RESULTS AND DISCUSSION

3.1 Identified mangrove species characteristics

The species we found in the research points are shown in Figure 5. The data were collected at 40 points in this study, which contain of 30 points (75%) to develop the AGC model, and 10 points (25%) to assess the accuracy. Determined sampling points based on the physical character variations so that the optimum predictions from a limited sample were obtained.

We identified five mangrove species at the research location in Benoa Bay. The species were *Rhizophora apiculata* (dominant at 11 points), *Rhizophora mucronata* (dominant at 10 points), *Sonneratia alba* (dominant at 18 points), *Xylocarpus granatum* (dominant at 1 point), and *Bruguiera gymnorhiza* (not dominant). *Rhizophora sp.* is frequently founded at the research location by Cerón-Souza et al., (2010) that *Rhizophora sp.* was the most well-known species in tropical coastal mangrove ecosystems.

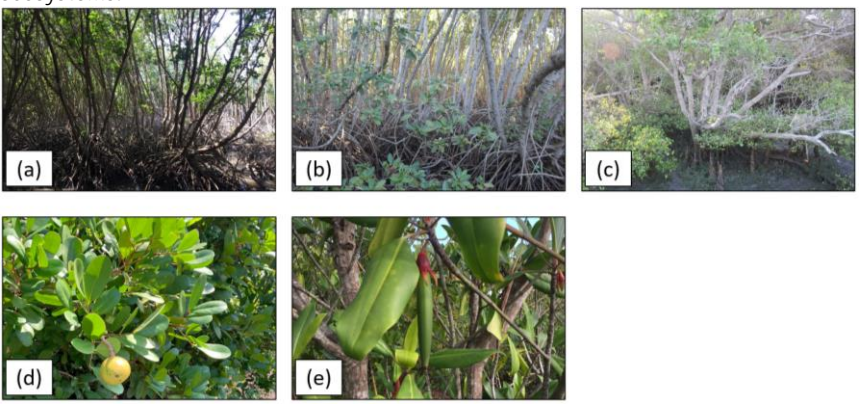

Figure 5. Mangrove species at coastal study in Benoa Bay; (a) *Rhizophora apiculata*, (b) *Rhizophora mucronata*, (c) *Sonneratia alba*, (d) *Xylocarpus granatum*, and (e) *Bruguiera gymnorhiza*

The DBH size varies, ranging from 6.43 cm (*Xylocarpus granatum*) to 55.1 cm (*Sonneratia alba*). The dominant *Rhizophora apiculata* and *Rhizophora mucronata* had the highest average DBH: 29.3 cm and 28.85 cm. According to Komiyama et al., (2008), *Rhizophora apiculata* has a higher density and DBH than *Rhizophora mucronata*. In this study, the AGC measurement ignored the tree height and canopy density parameters but used DBH parameters. The DBH variable provides an accurate estimation for biomass measurement (Abdul-Hamid et al., 2022).

3.2 Image classification and extraction of mangrove forests

The differences between mangrove and non-mangrove objects on Sentinel-2 composite RGB false colour (NIR, SWIR, red) images are shown in Figure 6. Mangrove objects are dark brown because they have relatively high values of NIR, SWIR, and red bands compared to other objects. According to Wang et al., (2018), the NIR and red bands are sensitive to the greenness of the vegetation, while according to Sadeghi et al., (2015), the SWIR bands are sensitive to soil moisture levels (mangrove habitat is affected by tides).

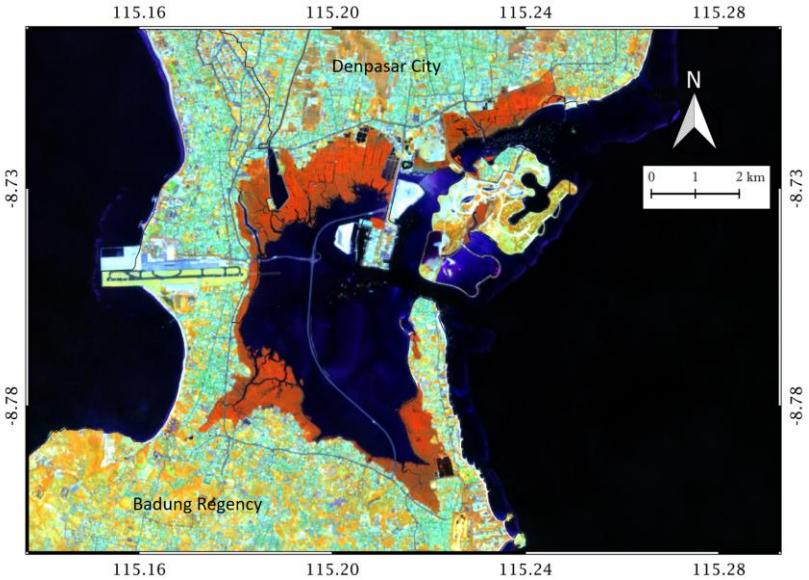

Figure 6. Mangrove view (in red colour) from composite RGB false colour (bands of NIR, SWIR, red) of Sentinel-2 data

This research focused on the mangroves in the coast of Benoa Bay, Bali Province. The satellite images were Sentinel-2 cloud-free composite (January–December 2020). The mangrove area was detected at the research location around 1,134.92 ha (Figure 7). The classification of mangrove and non-mangrove using the RF method based on several parameters has relatively high results, namely Overall Accuracy (OA) of 0.984 and kappa coefficient of 0.961.

The classification outcomes based on the Sentinel-2 image show substantial agreement with the field data, as indicated by the kappa coefficient (Dan et al., 2016). The high value of accuracy in the classification results was due to the use of limited classes (mangrove and non-mangrove), determination of uniform sample points (Dong et al., 2020), tidal duration, and percentage of cloud cover (Nguyen et al., 2020). Using multi-parameters with good sensitivity for mangrove forest detection in the RF classification process was proven to increase the accuracy during the classification process.

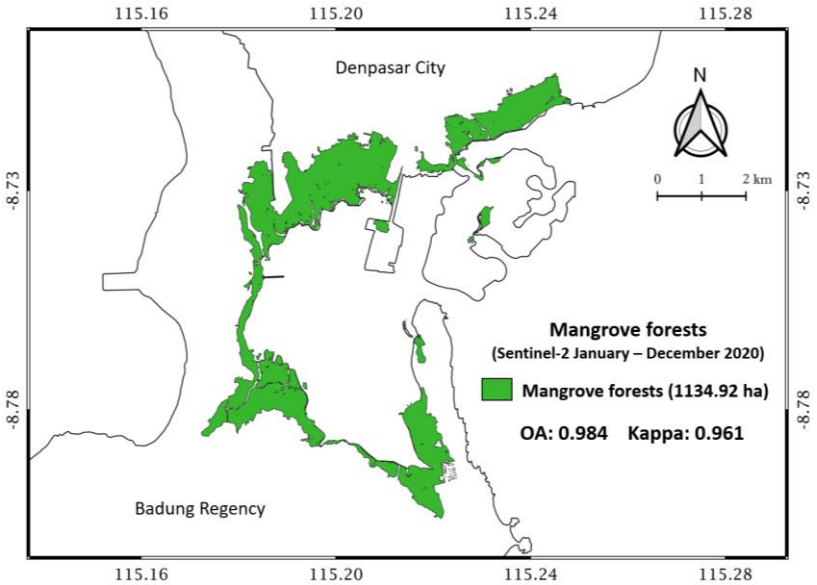

Figure 7. The extent of mangrove forests generated from Sentinel-2 (composite period January – December 2020) over the coasts of Benoa Bay, Bali Province

3.3 Above-ground Carbon Stocks

The calculation of AGB and AGC at the sample points is shown in Table 4. Based on these results, point 13 has the highest AGC value (175.77 tons/ha) among other sampling points, while point 23 has the lowest AGC value (29.77 tons/ha). The AGC estimation model was built assuming that AGB is closely related to tree diameter (DBH) and wood density. AGB affects the amount of AGC stored in each tree, so an increase in biomass is positively correlated with an increase in carbon (Purnamasari et al., 2021).

Table 4. Biomass and carbon stock calculation results

Data grouping	Sample Points	AGB (ton/ha)	AGC (ton/ha)	Dominant species
Model (75%)	1	67.70	31.82	*S. alba*
	2	74.38	34.96	*S. alba*
	3	229.18	107.72	*S. alba*
	4	157.76	74.15	*S. alba*
	5	210.05	98.72	*S. alba*
	6	193.95	91.15	*S. alba*
	7	171.12	80.43	*S. alba*
	8	279.32	131.28	*S. alba*
	9	73.96	34.76	*S. alba*
	10	129.27	60.75	*R. apiculata*
	11	262.63	123.44	*R. mucronata*
	12	242.87	114.15	*R. mucronata*
	13	373.98	175.77	*R. mucronata*
	14	156.81	73.70	*S. alba*
	15	116.53	54.77	*S. alba*
	16	215.19	101.14	*R. apiculata*
	17	173.13	81.37	*S. alba*
	18	188.99	88.83	*R. mucronata*
	19	166.03	78.03	*R. apiculata*
	20	205.46	96.57	*R. mucronata*
	21	280.85	132.01	*R. mucronata*

Data grouping	Sample Points	AGB (ton/ha)	AGC (ton/ha)	Dominant species
	22	123.31	57.96	*R. mucronata*
	23	63.34	29.77	*R. mucronata*
	24	79.84	37.52	*R. apiculata*
	25	147.75	69.44	*R. apiculata*
	26	159.25	74.85	*R. apiculata*
	27	261.76	123.03	*R. mucronata*
	28	309.94	145.67	*S. alba*
	29	79.16	37.21	*X. granatum*
	30	68.05	31.98	*R. apiculata*
Validation (25%)	31	178.45	83.87	*S. alba*
	32	133.52	62.75	*R. apiculata*
	33	211.09	99.21	*S. alba*
	34	74.48	35.01	*S. alba*
	35	223.38	104.99	*S. alba*
	36	90.09	42.34	*R. apiculata*
	37	126.44	59.43	*R. apiculata*
	38	335.24	157.56	*R. mucronata*
	39	193.49	90.94	*S. alba*
	40	156.85	73.72	*R. apiculata*

The species that dominated all sampling points were *Sonneratia alba*, but the highest AGC value was found at sample points dominated by *Rhizophora mucronata* species. These results are by Iksan et al., (2019) and Purnamasari et al., (2021), where *Rhizophora sp.* has higher biomass and carbon than other species. The amount of carbon stock in mangrove stands is influenced by DBH, biomass density, and canopy cover (Suwa et al., 2021). Based on observations at the study site, canopy cover at the sample point of *Rhizophora mucronata* dominance was higher than at the sample point of *Sonneratia alba* dominance.

3.4 Relationship of field biomass and sentinel image data, and model assessment

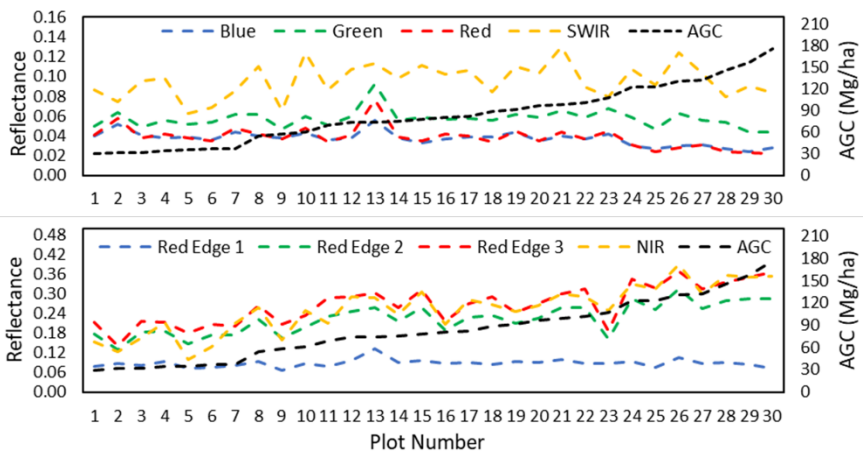

Figure 8. Relationships of observed AGC with Sentinel-2 multispectral bands in the visible, red edge, and infrared regions. Plots were arranged from nil to high carbon

The relationship between field AGC and Sentinel-2 multispectral band (visible, red edge, and infrared) are shown in Figure 8. Visible bands (blue, green, red), red edge 1, and SWIR have a relatively low relationship to AGC, even visible bands have an inverse relationship. Red edge 2, red edge 3, and NIR have a reasonable correlation with AGC

ranging from 0.8 to 0.86. However, the relationship of multispectral bands (red edge 2, red edge 3, NIR) with field AGC has a minor prediction error ranging from 16.51 Mg/ha to 20.04 Mg/ha (Table 4), so the resulting model has not had good enough.

The relationship between field AGC and several vegetation indices are shown in Figure 9. The vegetation index used was based on red edge and NIR bands which have sensitivity in vegetation detection (Nguy-Robertson et al., 2014; Imran et al., 2020). All vegetation indices correlate well with field AGC, ranging from 0.82 to 0.89. IRECI was the best vegetation index because it has a prediction error of 13.72 Mg/ha (Table 4).

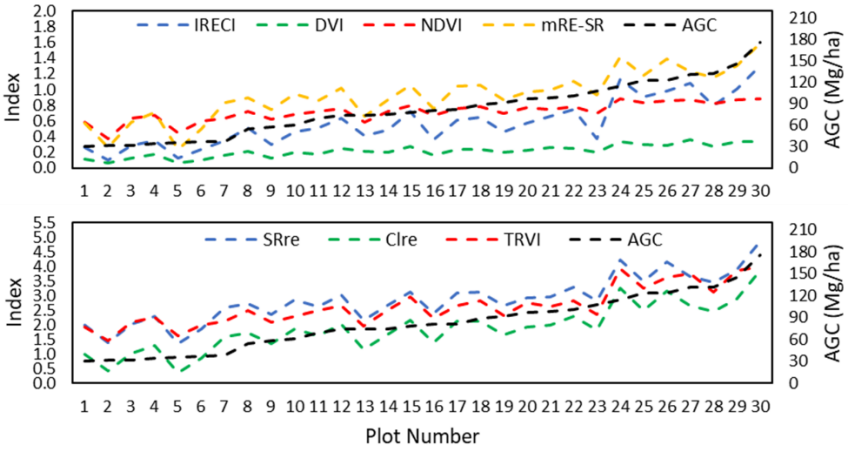

Figure 9. Relationship of observed AGC with Sentinel-2 derived vegetation indices. Plots were arranged from nil to high carbon

The red edge band is sensitive to vegetation's biophysical parameters, so it was good at detecting the vegetation index value (Zhu et al., 2017). The existence of the red edge band on Sentinel-2 can also be used to assess vegetation health (Goswami et al., 2021). High chlorophyll will absorb more energy in the 670-760 nm spectrum (Curran et al., 1995). In the electromagnetic spectrum, the red edge was located between the red band and NIR band, where there was a rapid change in the reflectance of vegetation in the spectrum.

In this research, a model was made using the combination of vegetation index to reduce the prediction error value. We also divided the combination of the vegetation index into two parts, namely the vegetation index with red edge bands and the vegetation index without red edge bands. The combination of vegetation indices resulted in a good correlation ranging from 0.88 to 0.89 (Table 5). The combination of IRECI and TRVI was the best, with an 11.09 Mg/ha prediction error. Meanwhile, the best combination of vegetation index without a red edge band was TRVI and DVI, with a prediction error of 13.63 Mg/ha.

The division of the combination of vegetation indices with red edge band and without red edge bands was done to provide an alternative to using optical satellite images that do not yet provide red edge bands (Landsat, SPOT, Planet Scope, etc.) in AGC estimation. However, adding a red edge band in the AGC estimation can give better results. According to Sibanda et al., (2015) and Dube et al., (2018), the red edge and NIR band also have strongly correlate with biomass which is the basis for calculating AGC. We hope that in further developments, the red edge band can be applied to all-optical satellite images.

Table 5. Correlation of observed AGC and Sentinel-2-based predictors

Modeling group	Predictor/s	Correlation with carbon, r	Agreement / correlation of observed and predicted value, r	Model prediction error, RMSE (Mg ha^{-1})
Sentinel-2 multispectral bands	Blue	-0.68	0.24	42.51
	Green	-0.15	-0.07	27.81
	Red	-0.57	0.26	31.89
	Red Edge 1	0.10	0.38	25.34
	Red Edge 2	0.80	0.91	18.31
	Red Edge 3	0.81	0.93	16.51
	NIR	0.86	0.91	20.04
	SWIR	0.19	0.35	26.04
Sentinel-2 derived vegetation indices	NDVI	0.82	0.76	18.65
	TRVI	0.88	0.78	18.57
	mRE-SR	0.87	0.78	18.19
	Clre	0.89	0.77	18.12
	SRre	0.89	0.77	18.12
	DVI	0.88	0.93	13.97
	IRECI	0.89	0.89	13.72
Combination of sentinel-2 derived vegetation indices	NDVI, TRVI	0.88	0.89	15.73
	TRVI, DVI	0.88	0.93	13.63
	IRECI, DVI	0.88	0.95	11.24
	NDVI, IRECI	0.89	0.95	11.22
	IRECI, TRVI	0.88	0.95	11.09

3.5 Mangrove carbon predictive mapping

The model with the best algorithm (lowest RMSE and highest r) was then used to estimate and map AGC values in the entire research area. The model with the best algorithm is shown in the following equation:

- Sentinel-2 vegetation index (IRECI and TRVI) derived AGC:
  $$\boldsymbol{AGC = 13.99 + 104.741 * IRECI + 3.025 * TRVI} \quad (1)$$
- Sentinel-2 vegetation index (TRVI and DVI) derived AGC:
  $$\boldsymbol{AGC = -33.385 + 27.576 * TRVI + 201.012 * DVI} \quad (2)$$

The AGC distribution derived from the Sentinel-2 vegetation indices model with red edge bands (IRECI and TRVI) and the Sentinel-2 vegetation index model without red edge bands (TRVI and DVI) is presented in Figure 10. AGC (IRECI and TRVI) range from 21.39 Mg/ha to 214.1 Mg/ha, while AGC (TRVI and DVI) range from 8.02 Mg/ha to 181.79 Mg/ha. These results are by Mahasani et al., (2021) at the exact location with an estimated AGC value range of 0 to 234.55 Mg/ha.

The estimated spatial distribution of AGC was by the results of field observations. The high value of predicted AGC was found in the middle of mangrove forests, where mangroves with dense canopy (dominant species: *Rhizophora sp.*). Likewise, low AGC was predicted to be at the edge of mangrove forests (near the sea and land) where mangroves with sparse canopy are found (species dominance: *Sonneratia sp.*).

The accuracy assessment of the Sentinel-2-based AGC prediction maps reveals that their prediction error (RMSE) value ranges from 11.09 Mg/ha to 16.51 Mg/ha, as presented in Figure 11. The lowest prediction error was the model developed based on combination of sentinel-2 derived vegetation indices (IRECI and TRVI: 11.09 Mg/ha, TRVI and DVI: 13.63 Mg/ha). The overall map accuracy ranged from 89% (Sentinel-2 derived vegetation indices map) to 95.3% (combination Sentinel-2-derived vegetation indices map). Correlation coefficient/agreement (r) between measured and predicted

biomass computed at 0.93, 0.89, 0.93 and 0.95 for models derived from Sentinel multispectral band, Sentinel-2 derived vegetation indices (IRECI), combination Sentinel-2 derived vegetation index (TRVI and DVI), and the combination Sentinel-2 derived vegetation index (IRECI and TRVI), respectively.

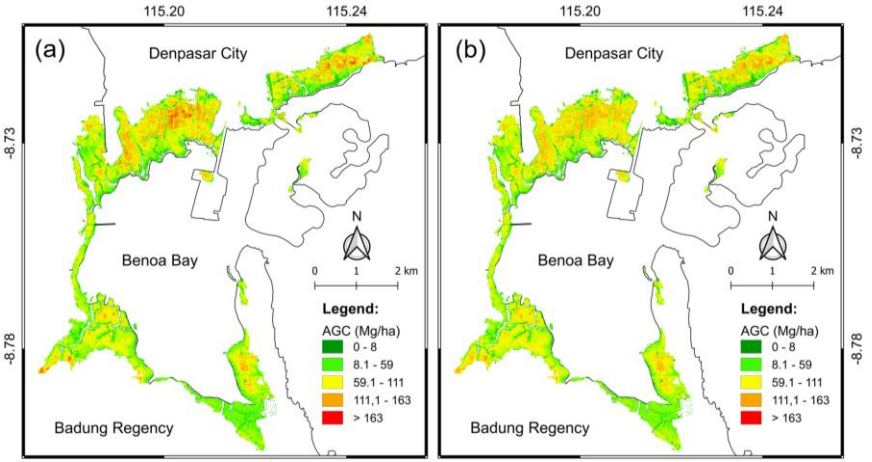

Figure 10. Predicted maps of AGC distribution in the study site derived from carbon models from (a) Sentinel-2 vegetation index IRECI and TRVI (eq. 1) and (b) Sentinel-2 vegetation index TRVI and DVI (eq. 2)

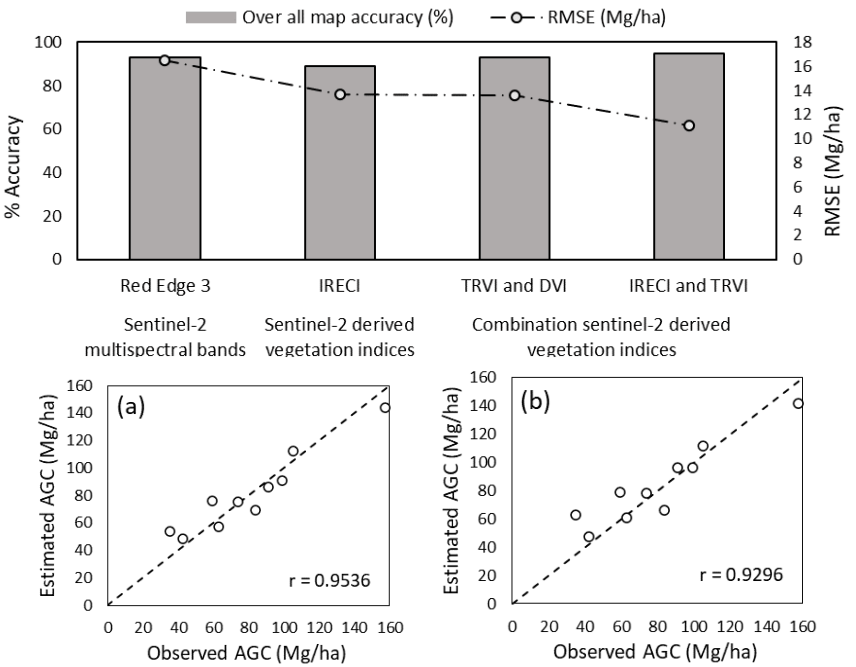

Figure 11. Accuracy assessment of predicted AGC distribution maps produced from the three Sentinel-based models (top panel). Scatter plots of observed and predicted AGC values correspond to (a) Sentinel-2 vegetation index IRECI and TRVI based map, (b) Sentinel-2 vegetation index TRVI and DVI based map. Dotted lines are 1:1 correspondence between observed and predicted AGC values

The model based on the combination of IRECI and TRVI derived from the Sentinel-2 image in this study was able to provide vital accuracy in the prediction of AGC. Agreement/correlation of predicted and observed AGC values combination IRECI and TRVI model was 0.95. The results of this study were able to increase the accuracy of the previous study (Sentinel-2 image) developed by Castillo et al., (2017). This study also has better accuracy compared to similar studies using optical images, as reported by Suardana et al., (2022) using Sentinel-2 images (0.77), Pham & Brabyn, (2017) using SPOT images (0.85), Wicaksono et al., (2016) using ALOS VNIR images (0.83), Jachowski et al., (2013) used GeoEye images (0.81), Proisy et al., (2007) used IKONOS images (0.93), and Li et al., (2007) used Landsat images (0.67). Using a combination of red edge and NIR bands is very helpful in increasing the accuracy of the AGC model, where the band is susceptible to detecting vegetation density.

4. CONCLUSION

In this study, five mangrove species were found in the observation points. The dominant species was *Rhizophora sp.*, which contributes to high AGC. The multivariate random forest algorithm has shown promising results in identifying mangrove ecosystems (OA = 0.984; kappa = 0.961). Overall, Sentinel-2 imagery has potential for mangrove AGC estimation and mapping. Based on the validation test result, the combination model of the IRECI and TRVI vegetation indices has the lowest prediction error of 11.09 Mg/ha. This study also validated the AGC model without red edge bands with the lowest prediction error results in the combination model of the vegetation index TRVI and DVI, which was 13.63 Mg/ha. The use of red edge and NIR bands is highly recommended in building the AGC model because it can increase accuracy. Furthermore, the results of this model are recommended to be tested in locations with different characteristics of mangrove forests and developed in measurements of below-ground carbon and soil so that further accuracy will be known for all estimates of mangrove forest carbon stocks. In addition, this model can be further developed in the future, not only for mapping mangrove and non-mangrove areas but also their composition, where the zonation of major or dominant mangrove species can be mapped. Finally, the developed model offered in the current study will be helpful for stakeholders and researchers concerned about carbon management in the wetland forest area.

Author Contributions: Author 1, 2, & 3: conceptualization, methodology, investigation, field survey, visualization and writing the original draft; Author 4: methodology, field survey, and investigation; Author 5: conceptualization, field survey, reviewing the writing, and editing the finalized manuscript; Author 6: methodology, investigation, field survey, and writing the original draft; Author 7: methodology and investigation; Author 8 & 9: reviewing the writing and editing the finalized manuscript; Author 10: QC, reviewing the writing and editing the finalized manuscript.

Competing Interests: The authors declare no conflict of interest.

Acknowledgements: This research is funded by Research Organization for Aeronautics and Space, National Research and Innovation Agency (ORPA, BRIN). The authors also would like to express the most profound appreciation to all field personnel and local people in Benoa Bay Bali for their assistance. We also appreciate the anonymous reviewers of the paper for their helpful and constructive comments. The authors also thank the Ngurah Rai Forest Park (Tahura Ngurah Rai) Bali for supporting us.

REFERENCES

Abdul-Hamid, H., Mohamad-Ismail, F. N., Mohamed, J., Samdin, Z., Abiri, R., Tuan-Ibrahim, T. M., ... & Naji, H. R. (2022). Allometric equation for aboveground

biomass estimation of mixed mature mangrove forest. *Forests, 13*(2), 1–18. https://doi.org/10.3390/f13020325

Alongi, D. M. (2012). Carbon sequestration in mangrove forests. *Carbon Management*, *3*(3), 313–322. https://doi.org/10.4155/cmt.12.20

Breiman, L. (2001). Random Forests. *Machine Learning*, *45*, 5–32. https://doi.org/10.14569/ijacsa.2016.070603

Brown, S. (2002). Measuring carbon in forests: Current status and future challenges. *Environmental Pollution*, *116*(3), 363–372. https://doi.org/10.1016/S0269-7491(01)00212-3

Castillo, J. A. A., Apan, A. A., Maraseni, T. N., & Salmo, S. G. (2017). Estimation and mapping of above-ground biomass of mangrove forests and their replacement land uses in the Philippines using Sentinel imagery. *ISPRS Journal of Photogrammetry and Remote Sensing*, *134*, 70–85. https://doi.org/10.1016/j.isprsjprs.2017.10.016

Cerón-Souza, I., Rivera-Ocasio, E., Medina, E., Jiménez, J. A., McMillan, W. O., & Bermingham, E. (2010). Hybridization and introgression in new world red mangroves, Rhizophora (Rhizophoraceae). *American Journal of Botany*, *97*(6), 945–957. https://doi.org/10.3732/ajb.0900172

Chai, T., & Draxler, R. R. (2014). Root mean square error (RMSE) or mean absolute error (MAE)? -Arguments against avoiding RMSE in the literature. *Geoscientific Model Development*, *7*(3), 1247–1250. https://doi.org/10.5194/gmd-7-1247-2014

Clevers, J. G. P. W., Jong, S. M. De, Epema, G. F., Addink, E. a, & Box, P. O. (2000). Meris and the Red-Edge Index. *2nd EARSeL Workshop, Enschede*.

Curran, P. J., Windham, W. R., & Gholz, H. L. (1995). Exploring the relationship between reflectance red edge and chlorophyll concentration in slash pine leaves. *Tree Physiology*, *15*(3), 203–206. https://doi.org/10.1093/treephys/15.3.203

Dan, T. T., Chen, C. F., Chiang, S. H., & Ogawa, S. (2016). Mapping and Change Analysis in Mangrove Forest By Using Landsat Imagery. *ISPRS Annals of Photogrammetry, Remote Sensing and Spatial Information Sciences*, *III–8*(July), 109–116. https://doi.org/10.5194/isprsannals-iii-8-109-2016

Dewanti, L. P. P., Subagiyo, & Wijayanti, D. P. (2020). Analysis of Biomass and Stored Carbon Stock in Mangrove Forest Area, Taman Hutan Raya Ngurah Rai Bali. *Indonesian Journal of Fisheries Science and Technology*, *16*(3), 219–224.

Dong, S., Chen, Z., Gao, B., Guo, H., Sun, D., & Pan, Y. (2020). Stratified even sampling method for accuracy assessment of land use/land cover classification: a case study of Beijing, China. *International Journal of Remote Sensing*, *41*(16), 6427–6443. https://doi.org/10.1080/01431161.2020.1739349

Dube, T., Gara, T. W., Mutanga, O., Sibanda, M., Shoko, C., Murwira, A., … & Hatendi, C. M. (2018). Estimating forest standing biomass in savanna woodlands as an indicator of forest productivity using the new generation WorldView-2 sensor. *Geocarto International*, *33*(2), 178–188. https://doi.org/10.1080/10106049.2016.1240717

ESA. (2012). *Sentinel-2: ESA's Optical High-Resolution Mission for GMES Operational Services*.

ESA. (2015). Sentinel-2 User Handbook. In *ESA Standard Document Date* (Issue 1). https://doi.org/10.1021/ie51400a018

Fadaei, H., Suzuki, R., Sakai, T., & Torii, K. (2012). a Proposed New Vegetation Index, the Total Ratio Vegetation Index (Trvi), for Arid and Semi-Arid Regions. *The International Archives of the Photogrammetry, Remote Sensing and Spatial Information Sciences*, *XXXIX-B8* (September), 403–407. https://doi.org/10.5194/isprsarchives-xxxix-b8-403-2012

FAO. (2007). The world's mangroves 1980-2005. In *FAO Forestry Paper* (Vol. 153).

Foody, G. M., Cutler, M. E., McMorrow, J., Pelz, D., Tangki, H., Boyd, D. S., & Douglas, I. A. N. (2001). Mapping the biomass of Bornean tropical rain forest from remotely sensed data. *Global Ecology & Biogeography*, *10*(4), 379–387. https://doi.org/10.1046/j.1466-822X.2001.00248.x

Fourqurean, J. W., Johnson, B., Kauffman, J. B., Kennedy, H., Lovelock, C. E., Megonigal, J. P., Rahman, A., Saintilan, N., & Simard, M. (2019). Coastal Blue Carbon. *Habitat Conservation*, *Ci*, 860. http://www.habitat.noaa.gov/coastalbluecarbon.html

Fromard, F., Puig, H., Mougin, E., Marty, G., Betoulle, J. L., & Cadamuro, L. (1998). Structure, above-ground biomass and dynamics of mangrove ecosystems: New data from French Guiana. *Oecologia*, *115*(1–2), 39–53. https://doi.org/10.1007/s004420050489

Gitelson, A. A., Gritz, Y., & Merzlyak, M. N. (2003). Relationships between leaf chlorophyll content and spectral reflectance and algorithms for non-destructive chlorophyll assessment in higher plant leaves. *Journal of Plant Physiology*, *160*(3), 271–282. https://doi.org/10.1078/0176-1617-00887

Gitelson, A. A., Keydan, G. P., & Merzlyak, M. N. (2006). Three-band model for noninvasive estimation of chlorophyll, carotenoids, and anthocyanin contents in higher plant leaves. *Geophysical Research Letters*, *33*(11), 2–6. https://doi.org/10.1029/2006GL026457

Goswami, J., Das, R., Sarma, K. K., & Raju, P. L. N. (2021). Red Edge Position (REP), an Indicator for Crop Stress Detection: Implication on Rice (Oryza sativa L). *International Journal of Environment and Climate Change*, *December*, 88–96. https://doi.org/10.9734/ijecc/2021/v11i430396

Hallik, L., Kuusk, A., Lang, M., & Kuusk, J. (2019). Reflectance properties of hemiboreal mixed forest canopies with focus on red edge and near infrared spectral regions. *Remote Sensing*, *11*(14). https://doi.org/10.3390/rs11141717

Han, J., Kamber, M., & Pei, J. (2012). *Data Mining Concepts and Techniques* (3rd Edition). Elsevier. https://doi.org/10.1016/C2009-0-61819-5

Hastuti, A. W., Suniada, K. I., & Islamy, F. (2017). Carbon Stock Estimation of Mangrove Vegetation Using Remote Sensing in Perancak Estuary, Jembrana District, Bali. *International Journal of Remote Sensing and Earth Sciences (IJReSES)*, *14*(2), 137. https://doi.org/10.30536/j.ijreses.2017.v14.a2841

Heumann, B. W. (2011). Satellite remote sensing of mangrove forests: Recent advances and future opportunities. *Progress in Physical Geography*, *35*(1), 87–108. https://doi.org/10.1177/0309133310385371

Hirata, Y., Tabuchi, R., Patanaponpaiboon, P., Poungparn, S., Yoneda, R., & Fujioka, Y. (2014). Estimation of aboveground biomass in mangrove forests using high-resolution satellite data. *Journal of Forest Research*, *19*(1), 34–41. https://doi.org/10.1007/s10310-013-0402-5

Hong-wei, Z., Huai-liang, C., & Fei-na, Z. (2019). The Modification of Difference Vegetation Index (DVI) in middle and late growing period of winter wheat and its application in soil moisture inversion. *E3S Web of Conferences*, *131*. https://doi.org/10.1051/e3sconf/201913101098

Iksan, M., Al Zarliani, W. O. D., Nare, L., Hafidhawati, S., & Baena, F. (2019). Biomass and Carbon Uptake of Mangrove Forests Pohorua Village, Muna Regency. *International Journal of Applied Biology*, *3*(2), 57–64.

Imran, H. A., Gianelle, D., Rocchini, D., Dalponte, M., Martín, M. P., Sakowska, K., Wohlfahrt, G., & Vescovo, L. (2020). VIS-NIR, red-edge and NIR-shoulder based normalized vegetation indices response to co-varying leaf and Canopy structural traits in heterogeneous grasslands. *Remote Sensing*, *12*(14). https://doi.org/

10.3390/rs12142254

Indonesian National Standard (SNI). (2011). *Pengukuran dan Penghitungan Cadangan Karbon – Pengukuran Lapangan untuk Penaksiran Cadangan Karbon Hutan (Ground Based Forest Carbon Accounting)*.

Jachowski, N. R. A., Quak, M. S. Y., Friess, D. A., Duangnamon, D., Webb, E. L., & Ziegler, A. D. (2013). Mangrove biomass estimation in Southwest Thailand using machine learning. *Applied Geography*, *45*, 311–321. https://doi.org/10.1016/j.apgeog.2013.09.024

Jordan, C. F. (1969). Derivation of Leaf-Area Index From Quality of Light on Forest Floor. *Ecological Society of America*, *50*(4), 663–666. https://doi.org/205.133.226.104

Kauffman, J. B., & Cole, T. G. (2010). Micronesian mangrove forest structure and tree responses to a severe typhoon. *Wetlands*, *30*(6), 1077–1084. https://doi.org/10.1007/s13157-010-0114-y

Kauffman, J. B., & Donato, D. C. (2012). *Protocols for the measurement, monitoring and reporting of structure, biomass and carbon stocks in mangrove forests*. Working Paper 86. CIFOR, Bogor, Indonesia.

Komiyama, A., Ong, J. E., & Poungparn, S. (2008). Allometry, biomass, and productivity of mangrove forests: A review. *Aquatic Botany*, *89*(2), 128–137. https://doi.org/10.1016/j.aquabot.2007.12.006

Komiyama, A., Poungparn, S., & Kato, S. (2005). Common allometric equations for estimating the tree weight of mangroves. *Journal of Tropical Ecology*, *21*(4), 471–477. https://doi.org/10.1017/S0266467405002476

Kumar, L., & Mutanga, O. (2017). Remote sensing of above-ground biomass. *Remote Sensing*, *9*(9), 1–8. https://doi.org/10.3390/rs9090935

Li, X., Yeh, A. G. O., Wang, S., Liu, K., Liu, X., Qian, J., & Chen, X. (2007). Regression and analytical models for estimating mangrove wetland biomass in South China using Radarsat images. *International Journal of Remote Sensing*, *28*(24), 5567–5582. https://doi.org/10.1080/01431160701227638

Mahasani, I. G. A. I., Osawa, T., Adnyana, I. W. S., Suardana, A. A. M. A. P., & Chonnaniyah. (2021). Carbon stock estimation and mapping of mangrove forest using ALOS-2 PALSAR-2 in Benoa Bay Bali, Indonesia. *IOP Conference Series: Earth and Environmental Science*, *2*(1), 429–443. https://doi.org/10.1088/1755-1315/944/1/012044

Mahasani, I. I., Osawa, T., & Sandi Adnyana, I. W. (2021). Estimation and Mapping of Above Ground Biomass of Mangrove Forest Using Alos-2 Palsar-2 in Benoa Bay, Bali, Indonesia. *ECOTROPHIC : Jurnal Ilmu Lingkungan, 15*(1), 75. https://doi.org/10.24843/ejes.2021.v15.i01.p07

Murdiyarso, D., Purbopuspito, J., Kauffman, J. B., Warren, M. W., Sasmito, S. D., Donato, D. C., ... & Kurnianto, S. (2015). The potential of Indonesian mangrove forests for global climate change mitigation. *Nature Climate Change*, *5*(12), 1089–1092. https://doi.org/10.1038/ nclimate2734

Nguy-Robertson, A. L., Peng, Y., Gitelson, A. A., Arkebauer, T. J., Pimstein, A., Herrmann, I., ... & Bonfil, D. J. (2014). Estimating green LAI in four crops: Potential of determining optimal spectral bands for a universal algorithm. *Agricultural and Forest Meteorology*, *192–193*, 140–148. https://doi.org/10.1016/j.agrformet.2014.03.004

Nguyen, H. H., Tran, L. T. N., Le, A. T., Nghia, N. H., Duong, L. V. K., Nguyen, H. T. T., ... & Premnath, C. F. S. (2020). Monitoring changes in coastal mangrove extents using multi-temporal satellite data in selected communes, Hai Phong City, Vietnam. *Forest and Society*, *4*(1), 256–270. https://doi.org/10.24259/fs.v4i1.8486

Oshiro, T. M., Perez, P. S., & Baranauskas, J. A. (2012). How many trees in a random

forest? *Conference: 8th International Conference on Machine Learning and Data Mining in Pattern Recognition, MLDM 2012, Lecture Notes in Computer Science*, *7376 LNAI*(July 2012), 154–168. https://doi.org/10.1007/978-3-642-31537-4_13

Patil, V., Singh, A., Naik, N., & Unnikrishnan, S. (2015). Estimation of Mangrove Carbon Stocks by Applying Remote Sensing and GIS Techniques. *Wetlands*, *35*(4), 695–707. https://doi.org/10.1007/s13157-015-0660-4

Pearson, T., Walker, S., & Brown, S. (2005). *Sourcebook for Land use , Land-use change and forestry Projects*. Retrieved from https://www.winrock.org/wp-content/uploads/2016/03/Winrock-BioCarbon_Fund_Sourcebook-compressed.pdf

Pham, L. T. H., & Brabyn, L. (2017). Monitoring mangrove biomass change in Vietnam using SPOT images and an object-based approach combined with machine learning algorithms. *ISPRS Journal of Photogrammetry and Remote Sensing*, *128*, 86–97. https://doi.org/10.1016/j.isprsjprs.2017.03.013

Pham, T. D., Yoshino, K., Le, N. N., & Bui, D. T. (2018). Estimating aboveground biomass of a mangrove plantation on the Northern coast of Vietnam using machine learning techniques with an integration of ALOS-2 PALSAR-2 and Sentinel-2A data. *International Journal of Remote Sensing*, *39*(22), 7761–7788. https://doi.org/10.1080/01431161.2018.1471544

Proisy, C., Couteron, P., & Fromard, F. (2007). Predicting and mapping mangrove biomass from canopy grain analysis using Fourier-based textural ordination of IKONOS images. *Remote Sensing of Environment*, *109*(3), 379–392. https://doi.org/10.1016/j.rse.2007.01.009

Pu, R., & Landry, S. (2012). A comparative analysis of high spatial resolution IKONOS and WorldView-2 imagery for mapping urban tree species. *Remote Sensing of Environment*, *124*, 516–533. https://doi.org/10.1016/j.rse.2012.06.011

Purnamasari, E., Kamal, M., & Wicaksono, P. (2021). Comparison of vegetation indices for estimating above-ground mangrove carbon stocks using PlanetScope image. *Regional Studies in Marine Science*, *44*. https://doi.org/10.1016/j.rsma.2021.101730

Ramdani, F., Rahman, S., & Giri, C. (2018). Principal polar spectral indices for mapping mangroves forest in South East Asia: study case Indonesia. *International Journal of Digital Earth*, *12*(10), 1103–1117. https://doi.org/10.1080/17538947.2018.1454516

Regier, P., Duggan, M., Myers-Pigg, A., & Ward, N. (2023). Effects of random forest modeling decisions on biogeochemical time series predictions. *Limnology and Oceanography: Methods*, *21*(1), 40–52. https://doi.org/10.1002/lom3.10523

Richards, D. R., & Friess, D. A. (2016). Rates and drivers of mangrove deforestation in Southeast Asia, 2000-2012. *Proceedings of the National Academy of Sciences of the United States of America*, *113*(2), 344–349. https://doi.org/10.1073/pnas.1510272113

Rodriguez-Galiano, V. F., Ghimire, B., Rogan, J., Chica-Olmo, M., & Rigol-Sanchez, J. P. (2012). An assessment of the effectiveness of a random forest classifier for land-cover classification. *ISPRS Journal of Photogrammetry and Remote Sensing*, *67*(1), 93–104. https://doi.org/10.1016/j.isprsjprs.2011.11.002

Rouse, J. W., Haas, R. H., Schell, J. A., & Deering, D. W. (1973). Monitoring Vegetation Systems In The Great Plains With Erts. In *Remote Sensing Center*. https://doi.org/10.1021/jf60203a024

Sadeghi, M., Jones, S. B., & Philpot, W. D. (2015). A linear physically-based model for remote sensing of soil moisture using short wave infrared bands. *Remote Sensing*

of Environment, *164*, 66–76. https://doi.org/10.1016/j.rse.2015.04.007

Savage, N. H., Agnew, P., Davis, L. S., Ordóñez, C., Thorpe, R., Johnson, C. E., O'Connor, F. M., & Dalvi, M. (2013). Air quality modelling using the Met Office Unified Model (AQUM OS24-26): Model description and initial evaluation. *Geoscientific Model Development*, *6*(2), 353–372. https://doi.org/10.5194/gmd-6-353-2013

Sibanda, M., Mutanga, O., & Rouget, M. (2015). Examining the potential of Sentinel-2 MSI spectral resolution in quantifying above ground biomass across different fertilizer treatments. *ISPRS Journal of Photogrammetry and Remote Sensing*, *110*, 55–65. https://doi.org/10.1016/j.isprsjprs.2015.10.005

Sidik, F., Fernanda Adame, M., & Lovelock, C. E. (2019). Carbon sequestration and fluxes of restored mangroves in abandoned aquaculture ponds. *Journal of the Indian Ocean Region*, *15*(2), 177–192. https://doi.org/10.1080/19480881.2019.1605659

Suardana, A. M. A. P., Anggraini, N., Aziz, K., Nandika, M. R., Ulfa, A., Wijaya, A. D., ... & Dewanti, R. (2022). Biomass Estimation Model and Carbon Dioxide Sequestration for Mangrove Forest Using Sentinel-2 in Benoa Bay, Bali. *International Journal of Remote Sensing and Earth Sciences*, *19*(1), 91–100.

Suwa, R., Rollon, R., Sharma, S., Yoshikai, M., Albano, G. M. G., Ono, K., ... & Nadaoka, K. (2021). Mangrove biomass estimation using canopy height and wood density in the South East and East Asian regions. *Estuarine, Coastal and Shelf Science*, *248*(May), 106937. https://doi.org/10.1016/j.ecss. 2020.106937

Tucker, C. J. (1980). A spectral method for determining the percentage of green herbage material in clipped samples. *Remote Sensing of Environment*, *9*(2), 175–181. https://doi.org/10.1016/0034-4257(80)90007-3

Wang, B., Jia, K., Liang, S., Xie, X., Wei, X., Zhao, X., Yao, Y., & Zhang, X. (2018). Assessment of Sentinel-2 MSI spectral band reflectances for estimating fractional vegetation cover. *Remote Sensing*, *10*(12), 1–20. https://doi.org/10.3390/rs10121927

Wicaksono, P., Danoedoro, P., Hartono, H., Nehren, U., & Ribbe, L. (2011). Preliminary work of mangrove ecosystem carbon stock mapping in small island using remote sensing: above and below ground carbon stock mapping on medium resolution satellite image. *Remote Sensing for Agriculture, Ecosystems, and Hydrology XIII*, *8174*(October 2011), 81741B. https://doi.org/10.1117/12.897926

Wicaksono, P., Danoedoro, P., Hartono, & Nehren, U. (2016). Mangrove biomass carbon stock mapping of the Karimunjawa Islands using multispectral remote sensing. *International Journal of Remote Sensing*, *37*(1), 26–52. https://doi.org/10.1080/01431161.2015.1117679

World Agroforestry Center. (2022). *Wood density*. Accessed from http://db.worldagroforestry.org/wd

Zhu, Y., Liu, K., Liu, L., Myint, S. W., Wang, S., Liu, H., & He, Z. (2017). Exploring the potential of world view-2 red-edge band-based vegetation indices for estimation of mangrove leaf area index with machine learning algorithms. *Remote Sensing*, *9*(10). https://doi.org/10.3390/rs9101060